NPL
National Physical Laboratory

Report

NPL REPORT IR 10

Measuring quasi - mono-energetic neutron spectra with the NPL Time-of-Flight system

N P Hawkes, A Bennett and
N J Roberts

NOT RESTRICTED

MAY 2008

National Physical Laboratory | Hampton Road | Teddington | Middlesex | United Kingdom | TW11 0LW

Switchboard 020 8977 3222 | **NPL Helpline** 020 8943 6880 | **Fax** 020 8614 0446 | **www.npl.co.uk**

Department for **Innovation, Universities** & **Skills**

Measuring quasi-monoenergetic neutron spectra with the NPL Time-of-Flight system

N P Hawkes, A Bennett and N J Roberts
Quality of Life Division

ABSTRACT

Neutron spectra produced at NPL's quasi-monoenergetic neutron irradiation facility have been measured by the Time-of-Flight technique, and compared with calculations carried out using the TARGET code.

ISSN 1754-2952

National Physical Laboratory
Hampton Road, Teddington, Middlesex, TW11 0LW

Approved on behalf of the Managing Director, NPL, by Bajram Zeqiri,
Knowledge Leader, Acoustics & Ionising Radiation Team, authorised
by Martyn Sené, Director, Quality of Life Division

Contents

Figures

Tables

1 Introduction

The Monoenergetic Neutron Facility[1] at NPL produces neutron fields with a very narrow spread of energies (quasi-monoenergetic fields) for research and for detector calibrations. The neutrons are produced by directing an ion beam (protons or deuterons) from a Van de Graaff accelerator onto a neutron-producing target at the centre of a low-scatter experimental area. Recently a requirement has arisen to demonstrate that the neutron spectra from these targets are adequately monoenergetic, i.e. that there are no significant low energy components due (for example) to migration of the target nuclide into the backing material.

A suitable technique for measuring the spectra with sufficient resolution is Time-of-Flight (ToF), in which neutron energies are measured by timing the neutrons as they travel a known distance. The beam from the accelerator is divided into short pulses (such that the duration of each is essentially negligible), and a beam pickup device just upstream of the target detects such a pulse as it passes. A suitable neutron detector placed a known distance in front of the target registers the arrival of neutrons, and the time interval between the pulse signal and the neutron signal is used to derive the neutron energy.

During the 1980s a time-of-flight system was in use at the NPL Neutron facility, but this was taken out of use in 1990. Following a favourable report on the feasibility of re-commissioning the system[2], work was undertaken during the 2001 - 2004 DTI National Measurement System (NMS) Programme to reinstate the pulsing electronics in the Van de Graaff accelerator and the signal processing electronics in the Control Room. The aim of the work reported here, undertaken during the 2004 - 2007 NMS Programme, was to improve the timing resolution of the system and measure target spectra.

2 Basic operation of the NPL Time-of-Flight system

The NPL ToF system is shown schematically in Figure 1. Electronic modules are from the Ortec range unless stated, and model numbers are given. Abbreviations used are as follows: HV, high voltage; LV, low voltage; PM, photomultiplier; CF, constant fraction; DISC, discriminator; TAC, time-to-amplitude converter; SCA, single-channel analyser; MCA, multi-channel analyser.

2.1 Beam pulses

The beam pulses are generated by electronics within the high voltage terminal of the accelerator (not shown in Figure 1). The pulses are typically of about 5 ns duration, and the period is adjustable from 400 ns to 51.2 μs to allow for different target - detector flight path lengths.

2.2 Beam pulse pickup

The beam pickup is a capacitive device consisting of a short metal tube mounted coaxially inside the beam line but insulated from it. The signal is brought out via a vacuum-tight electrical feedthrough.

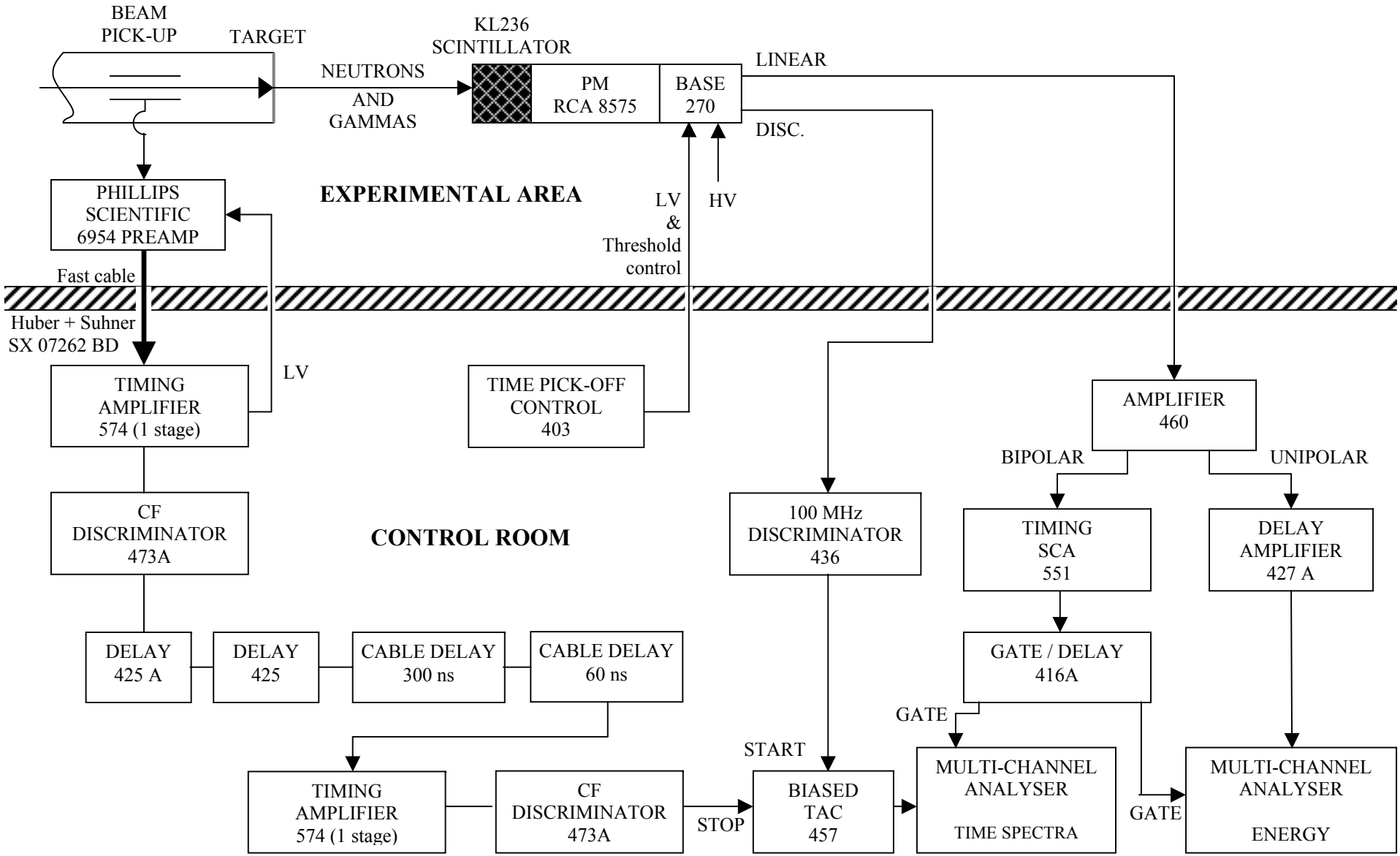

Figure 1. Arrangement of ToF electronics for plastic scintillator.

There are in fact two such beam pickups: the 'Target' pickup shown, used for timing, and another much further upstream, close to the output of the accelerator. This Accelerator pickup is used during setting up to optimise the beam pulser electronics.

2.3 Neutron detectors

Two different neutron detectors are available. A fast plastic scintillator (KL236, 1 inch in diameter by 1 inch long) is used for neutron energies above about 0.5 MeV, and in addition there is a lithium glass scintillator (NE912, 2 inches by 2 inches) suitable for neutrons below about 2 MeV.

Figure 1 shows the electronic arrangement for the plastic scintillator detector, which has a preamplifier and a constant fraction discriminator built into the photomultiplier base. The former produces a linear energy signal and the latter a timing pulse. The Model 403 Time Pickoff Control provides low voltage power to the active electronics in the photomultiplier base and also controls the discriminator threshold remotely.

The arrangement of the electronics for the second detector is very similar, except that the photomultiplier base is passive, and a separate preamplifier and discriminator have to be set up in the Experimental Area.

2.4 Start and Stop

As is usual for ToF systems, the timing device (TAC) is started by the signal from the neutron detector, and stopped by the signal from the pickup. This reversal of what one might expect is done to reduce dead time, the count rate from the neutron detector being typically much lower than the frequency of beam pulses. It is achieved by putting the pickup signal through a delay so that it arrives after the neutron signal. As a consequence of this arrangement, flight time increases from right to left in the ToF spectra displayed later in this report.

For best timing it is desirable that the TAC should be stopped by the same beam pulse as the one that generated the start event, rather than by an earlier or later pulse in the train of beam pulses. To ensure this, the required pickup signal delay was first estimated to better than half a beam period, based on an experimental measurement of the delay difference between the start and stop sides of the electronics. (This was obtained by taking a pulser into the Experimental Area and injecting pulses into start and stop sides simultaneously). The estimated value was then adjusted to place the ToF peaks in the desired positions in the measured spectra. As a check that the timing was based on the correct beam pulse, the pulse frequency was repeatedly divided by two, and confirmation obtained that the ToF peaks did not jump to a new position. Subsequent changes of experimental conditions (a different neutron energy, for example, or a different target - detector distance) necessitated changes to the delay, but these were straightforward to calculate from the known starting position.

The delay on the stop side is entirely passive, because of the experience of the designer of the original system that an active delay was prone to multiple pulsing[3]. The delays needed in some configurations are large (about 1000 ns), and active electronics is required at the end of the passive delay in order to recondition the signal pulse.

2.5 Discrimination thresholds

The timing discriminator built into the photomultiplier base is designed for good timing characteristics, but does not necessarily provide a well-defined amplitude threshold. In order to make the energy threshold of the system well defined, the linear signal from the photomultiplier base was passed via a spectrometry amplifier into a single-channel analyser (SCA), and the SCA output was in turn used to generate a gate signal that gated the ToF multi-channel analyser (MCA).

The energy spectrum from the detector was also acquired, by passing another output from the spectrometry amplifier to a second MCA (also gated with the output from the SCA).

2.6 Time calibration

The time scale is calibrated with an Ortec model 462 Time Calibrator (not shown in Figure 1). This device produces a series of peaks in the ToF spectrum with a well-defined separation. The peak positions are subsequently fitted to a straight line, and the slope of the line gives the MCA channel width in nanoseconds.

When the ToF system is in operation, all detected gammas coming directly from the target form a single peak that is easily distinguishable from the neutron events by virtue of the difference in flight time. This peak is very useful as a marker because, based on the known transit time for gammas, it allows the zero point on the time scale (corresponding to a notional flight time of zero) to be identified. Furthermore, as direct flight times for gammas can differ at most by the transit time across the scintillator, the shape of the peak gives a useful indication of the timing resolution of the system. In the present work, the peak shape was used directly as a resolution function, the transit time being negligible.

3 System developments

3.1 Beam pickup signals

It is essential to trigger reliably from the beam pickup. However, this proved surprisingly difficult to achieve.

Figure 2 shows the signals from the two beam pickups, displayed on a high speed digital oscilloscope (Tektronix TDS 5052). (The time delay between the two traces is arbitrary, and the blue pulses do not necessarily correspond to the yellow pulse immediately preceding.) It is clear that the signal-to-noise ratio has degraded considerably by the time the beam reaches the Target pickup. It is also striking that the pulse period is 200 ns; the setting of the pulser circuit, and the minimum it was constructed to produce, was 400 ns. This halving of the period was observed on several occasions and is clearly a problem with the pulser system inside the accelerator.

In Figure 3 the same signals are shown over a longer time interval. The frequency doubling is again evident, and this time there are indications that the signal is alternating between large and small pulses. This is especially evident in the blue (Target) trace, and makes reliable triggering difficult (particularly as the discriminator triggers on the negative-going lobe of the pulse). In Figure 4 the blue trace has been changed to show instead the output of the constant fraction discriminator connected to the Target pickup, and the two problems of missed triggers and spurious triggers are both evident. Spurious triggers produce spurious peaks in the ToF spectrum, and missed triggers have the effect of shifting the peaks to longer times by one beam pulse period. If the TAC range is not great enough to acquire these peaks, they are lost, and the efficiency of the system is reduced by an undetermined factor.

After considerable experimentation, the following changes were made to the system:

1. A preamplifier (Phillips Scientific model 6954) was installed at the shortest possible distance from the Target pickup. This preamplifier has a gain of 100 and a rise time of 220 ps. Previously the pickup signal was passed unmodified to an Ortec model 260 Time Pickoff unit in the Control Room.
2. Additional amplification was provided by one stage of an Ortec model 574 fast amplifier (gain approximately 4, no shaping) in the Control Room.
3. The cable between the Target pickup and the Control Room, 40 m long approximately, was changed from ultra high bandwidth Andrew Heliax HJ7-50A to high bandwidth Huber + Suhner SX 07262 BD. Although the new cable has a lower bandwidth than the old, it is much easier to handle, with no noticeable loss of performance for this application.

Table 1. Comparison of cable properties.

	HJ7-50A	SX 07262 BD	RG 58
2 GHz attenuation	0.0342 dB / m [4]	0.34 dB / m [5]	1.4 dB / m [6]
Outer dia. approx	50 mm	11 mm	5 mm

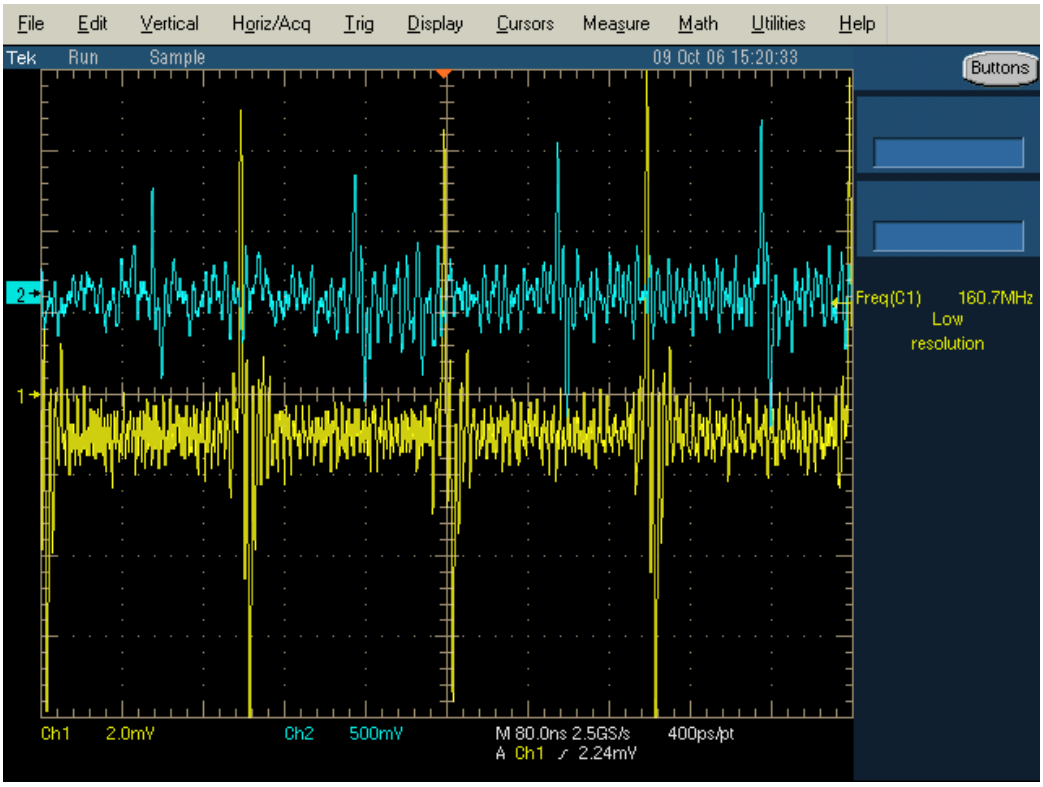

Figure 2. Beam pickup signals (yellow, Accelerator; blue, Target).

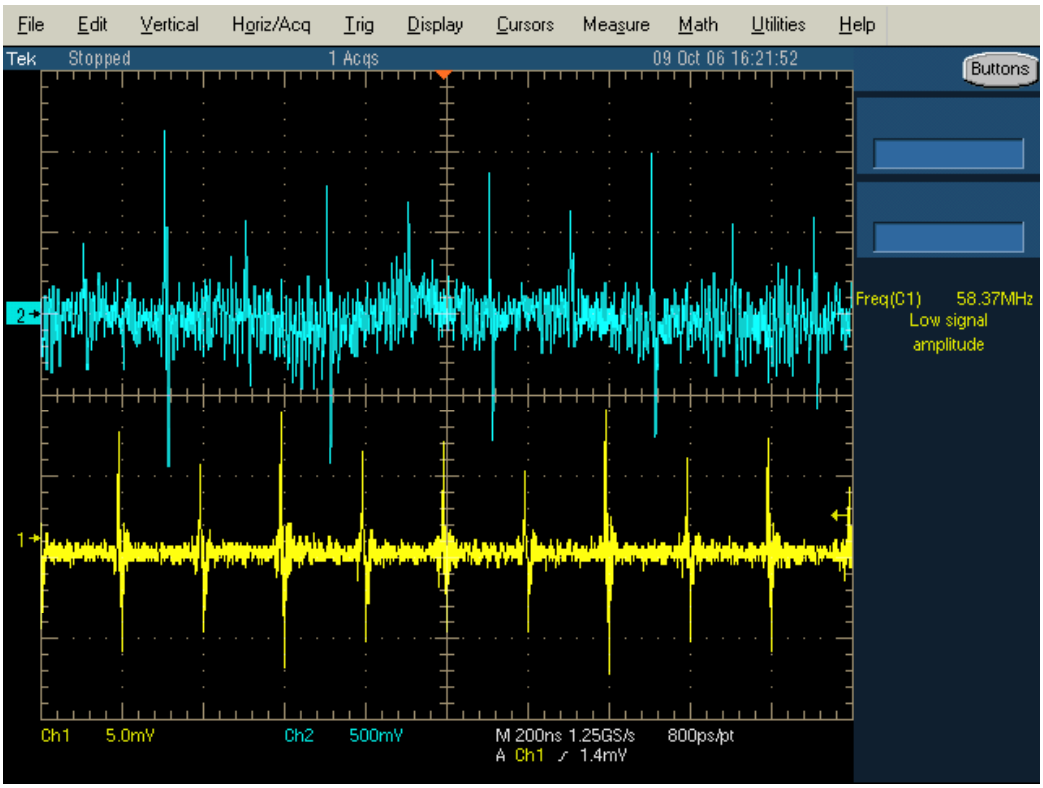

Figure 3. Pickup signals at twice the set frequency and showing alternation of signal amplitude.

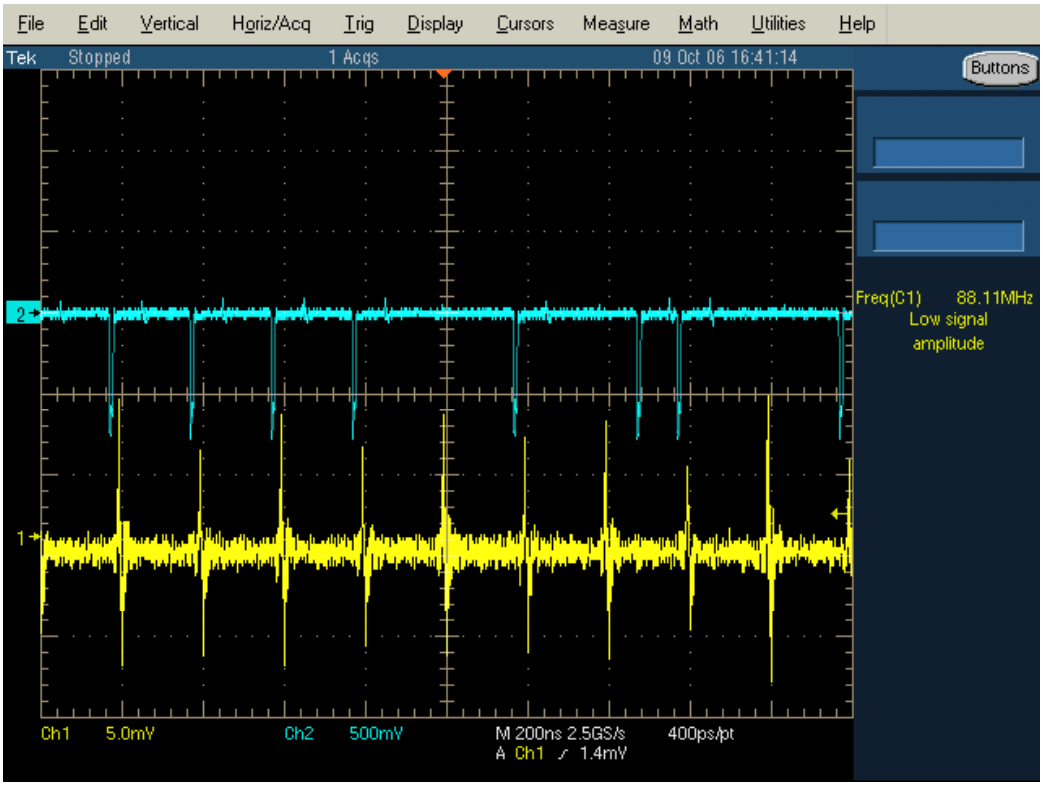

Figure 4. Missed and spurious triggers in the Target pickup signal (blue).

3.2 Beam pickup timing

In cases where, as here, the transit time of gamma rays across the detector is negligible, the gamma peak should be very narrow. However, this was often not the case. For example, Figure 5 shows the gamma peak shape observed under nominally identical conditions on two successive days in June 2006. The peak is very broad at the base in both cases, and in addition the shape has changed considerably from one day to the next.

As the timing properties of the detector seem unlikely to change, this variation is attributed to a change in the timing of the pickup pulse relative to the arrival of the bulk of the protons on the target, presumably as a result of changes in the time structure of the beam pulse. These time resolution problems affect the neutron peak as well, and shapes like those in the Figure would substantially impair the system's sensitivity to low-energy components in the neutron spectrum.

Many different adjustments to the electronics were tried in a search for better performance. For example, the operating mode of the first Constant Fraction (CF) discriminator on the stop side of the system was changed from CF to Leading Edge (LE), as it is understood that the advantage of CF over LE only applies over a limited range of rise times. At the same time, a programme of redesign and replacement of the pulser electronics within the accelerator was begun, and as at September 2007 only one original circuit board remains of the four that make up the system.

The spectra shown later in this report, acquired during the period November 2006 - February 2007, demonstrate substantial improvements in resolution over that evident in Figure 5, although some variation between nominally identical setups does remain.

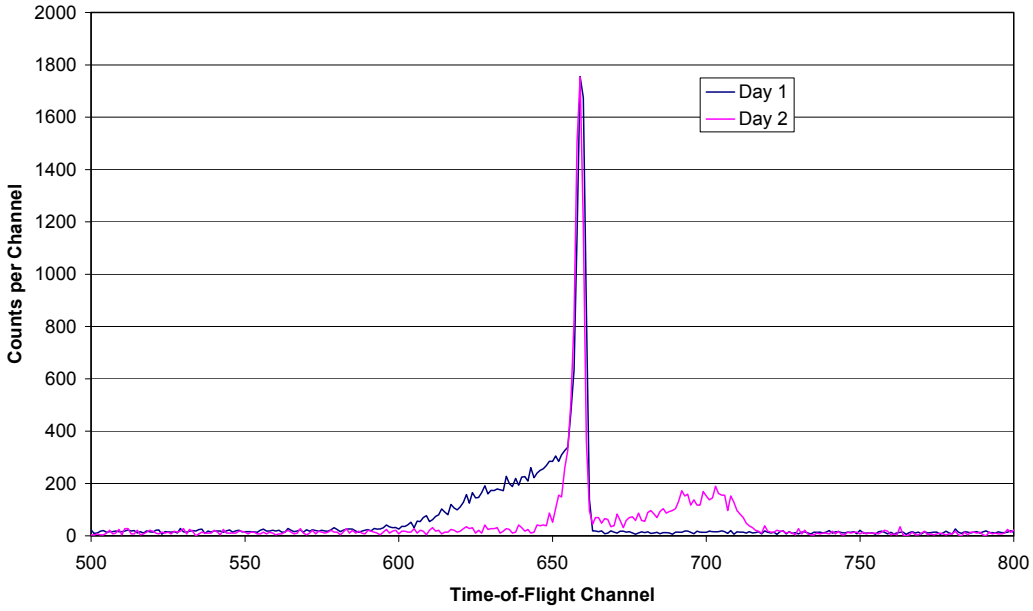

Figure 5. Gamma peak shape on two successive days, June 2006.

3.3 Energy measurements

In ToF spectrometry, the measured speed v of the particle is used to derive its kinetic energy K via the relation

$$K = m_0 (\gamma - 1) c^2$$

where

$$\gamma = 1 / (1 - v^2/c^2),$$

c is the speed of light, and m_0 is the rest mass of the particle. In early trials with the NPL system, using monoenergetic neutrons from the ^{7}Li(p, n) reaction, the neutron energy deduced from the ToF data was found to be significantly lower (by up to tens of keV) than that expected from the setting of the energy analysing magnet that controls the energy of the proton beam. This difference was seen for both types of detector (lithium glass and plastic), and led to the suggestion that the magnet calibration might be different for continuous (DC) and pulsed beams.

To investigate this, a threshold check using the ^{7}Li(p, n) reaction was carried out with both types of beam in quick succession. In this procedure, the analysing field is set to a value just below that corresponding to the reaction threshold energy of 1.8806 MeV, and then increased in small steps until neutrons appear. Extrapolating back to zero yield then gives the magnet setting that corresponds to the threshold.

Typical results from this exercise are shown in Figure 6, in which the magnet setting is expressed in terms of the frequency of the Nuclear Magnetic Resonance (NMR) servo that controls the magnet. Although there are some differences in threshold position from one run to the next, they are no larger than normally seen when performing repeat measurements with DC beams, and no systematic differences between DC and pulsed beams are evident. It was therefore concluded that the magnet calibration is independent of whether the beam is pulsed or not.

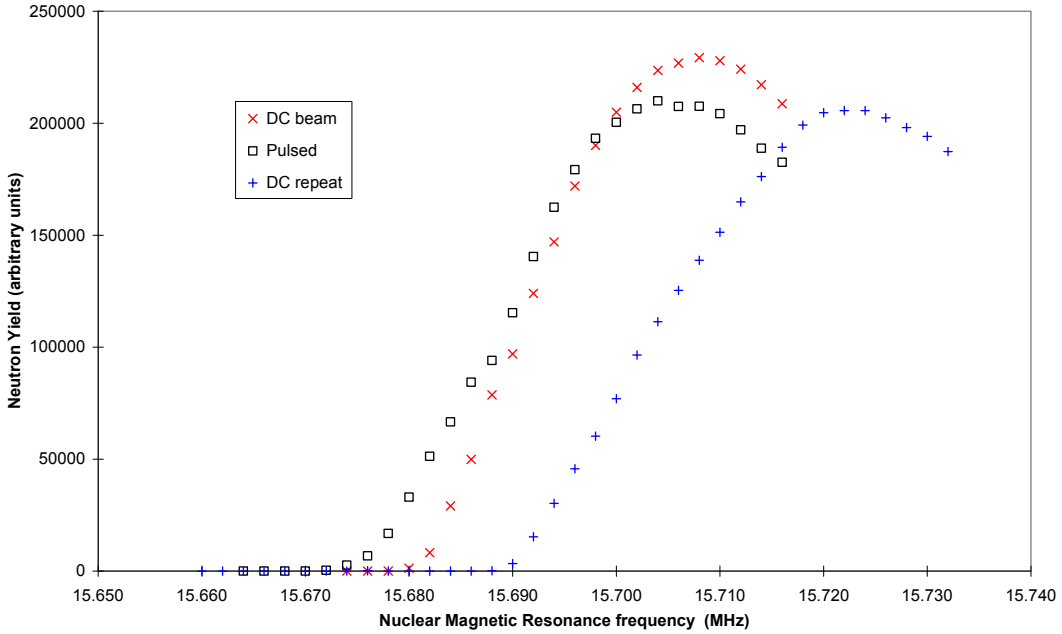

Figure 6. Energy calibration checks with DC and pulsed beams.

The size of typical discrepancies between the ToF and magnet energy values was observed to decrease as the ToF system was developed. Values as at late 2006 / early 2007 are given with the ToF spectra shown later in this report. The estimated uncertainties in the ToF energies are based on uncertainties of ± 0.5 - 0.7 channels in the positions of the peaks, and a ± 0.4 cm uncertainty in the total distance from the target to the effective centre of the detector (taken as the centre of the scintillator). Some of the discrepancies are now consistent with zero, but the tendency for ToF values to be lower than magnet values remains. In the light of the calibration checks, a genuine energy difference is unlikely, and the explanation probably lies in a systematic error in (for example) the TAC calibration or the location of the detector's effective centre. The energy calibration is not crucial for checking whether target spectra are monoenergetic.

4 Measured ToF Spectra

In this section, the results of three ToF measurements are presented and discussed. In all cases, neutrons were produced by directing a proton beam into a LiF target of nominal thickness 60 μg / cm^2, and making use of the ^{7}Li(p, n) reaction. Inscatter was measured by carrying out a run with a shadow cone blocking direct paths from target to detector, and the result was subtracted from the run with no cone. The total beam charge delivered to the target, as measured by a current integrator, was used to derive the appropriate normalisation for the shadow cone run.

The plastic scintillator was used for all the measurements presented here.

4.1 Run 1: ^{7}Li(p, n) with E_p = 2.922 MeV

At this proton energy the ^{7}Li(p, n) reaction generates two monoenergetic neutron lines: the n_0 (ground state) one at 1225.5 keV and the n_1 line at 745.8 keV (both energy values calculated by the program DROSG-2000[7]). For this reason the reaction is not normally used for metrology applications at this energy, but for the present work the second neutron line is a positive advantage as it provides additional ToF information.

Figure 7 shows the Total and Inscatter measurements on a log scale to allow the two to be compared. Vertical lines have been drawn at the observed positions of the inscatter-corrected peaks, and these lines show that (apart from features attributable to resolution) the inscatter peaks appear at longer flight times than the direct peaks, as one would hope. (Recall that flight time increases from right to left.) The 'late' gammas are assumed to be ones that have scattered and taken a longer path to the detector.

In Figure 8 the Total spectrum is shown over a wider time range, and the duplicate peaks due to missed stop pulses are clearly evident, the duplicated part of the spectrum containing a substantial 6% of the number counts in the main part. Had the time range of the TAC been extended further, more duplicate peaks, corresponding to successive missed stops, would probably have been visible. All duplicate peaks were disregarded in the analysis that follows.

The final ToF spectrum, corrected for inscatter, is shown in Figure 9. The gamma peak is reasonably narrow (FWHM 5.2 channels or 2.0 ns), and subtraction of the inscatter has left it strikingly symmetric. There is evidence of a small low-energy tail on the n_0 neutron peak, which could be an indication that some of the target lithium atoms have migrated into the thick backing of the target layer. The n_1 peak is too small to show evidence of a tail.

The neutron peaks in Figure 9 (and subsequent similar Figures) have been labelled with the energy expected from the magnet calibration and that deduced from the flight time. As mentioned earlier, differences are small, but the ToF energies are systematically lower than the magnet energies.

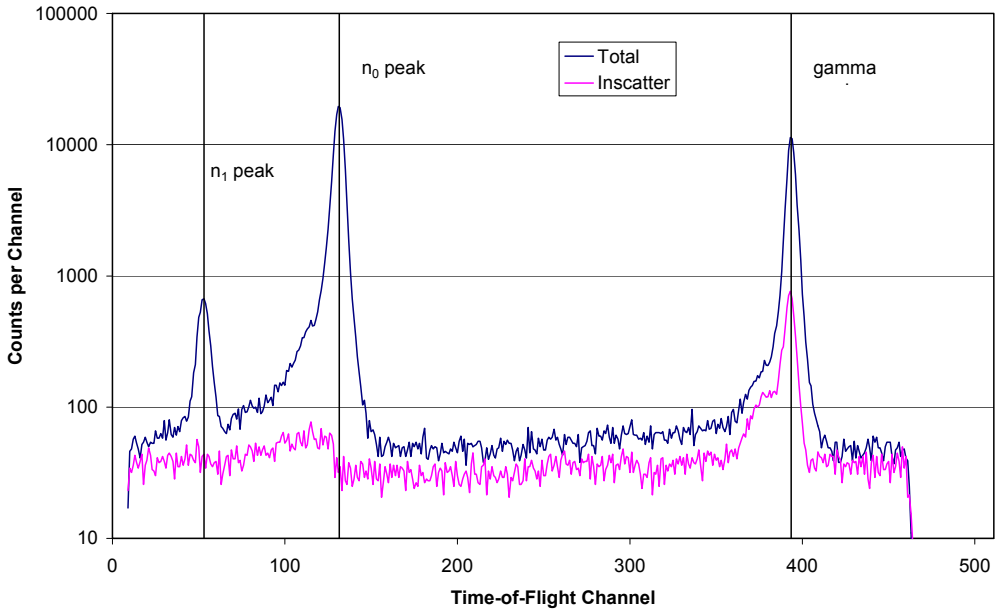

Figure 7. Run 1 (^{7}Li(p, n) ToF with E_p = 2.922 MeV), Total and Inscatter

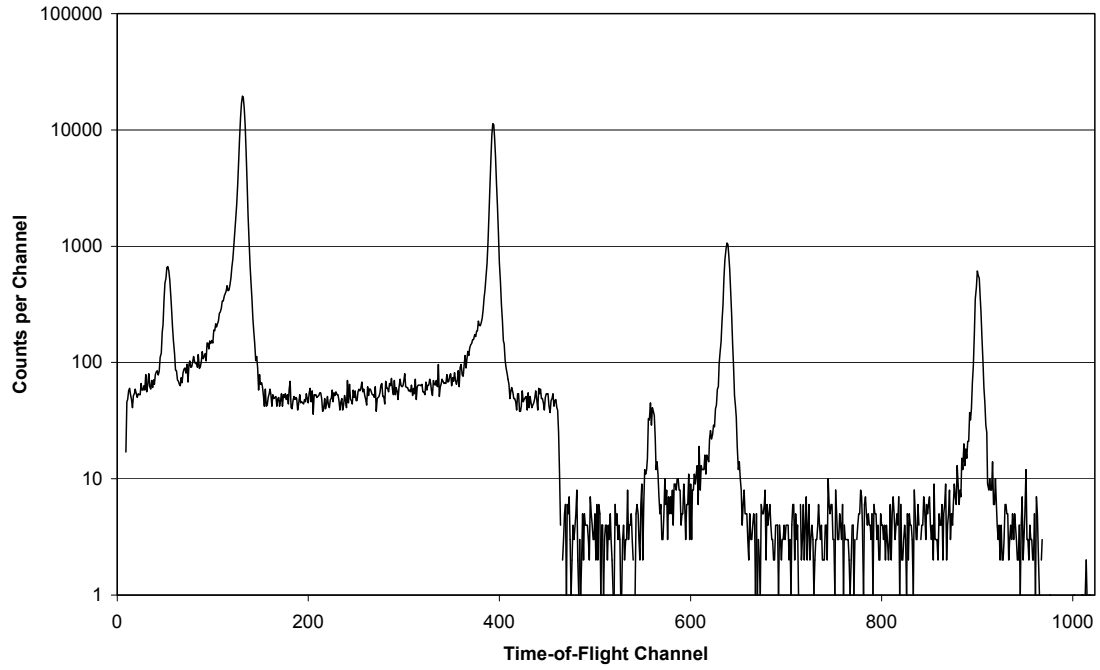

Figure 8. Run 1 Total spectrum at extended flight times.

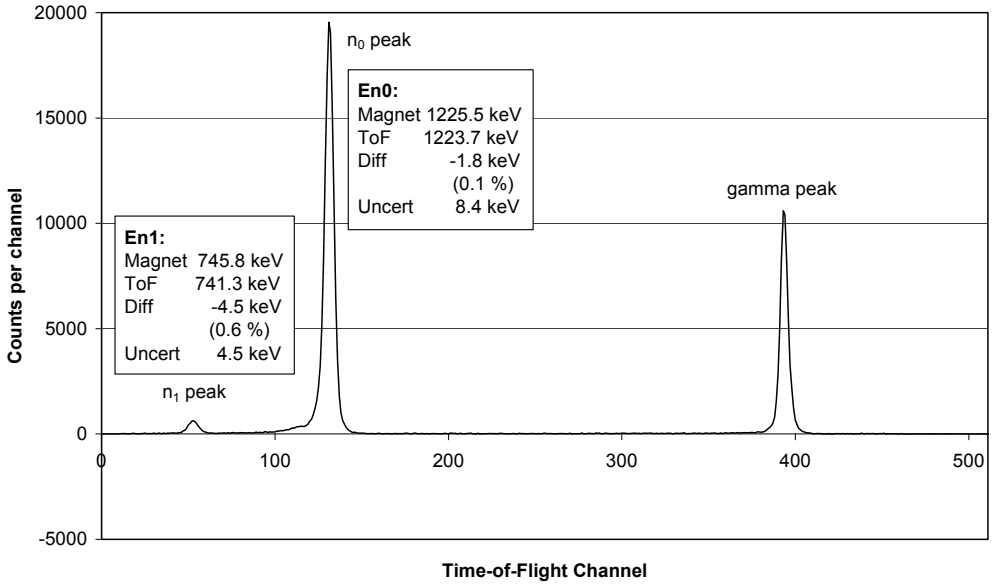

Figure 9. Inscatter-corrected ToF spectrum for Run 1.

4.2 Run 2: Repeat of Run 1

A repeat of Run 1 was carried out three months later to check reproducibility, and the results are shown below (Figure 10 and Figure 11).

This time the number of missed stops is negligible; the duplicated part of the Total spectrum (not shown in the Figures) contains only 0.006% of the counts in the main part. However, it is clear from Figure 10 that the time resolution is not as good as for Run 1, the base of the gamma peak being considerably wider this time.

As a consequence, it is harder to see low-energy neutrons in the corrected ToF spectrum (Figure 11).

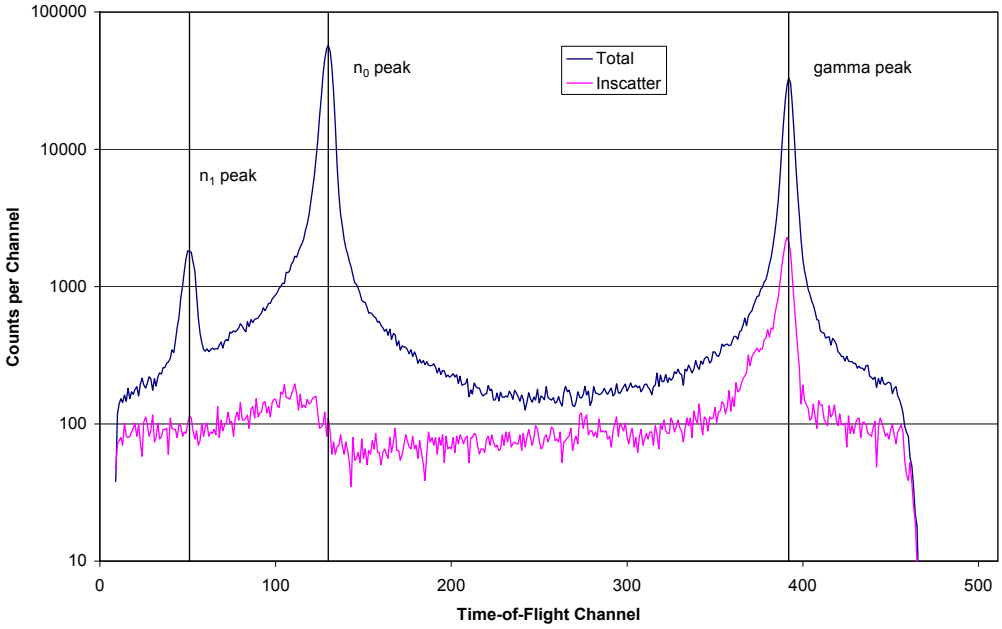

Figure 10. Total and Inscatter for Run 2 (repeat of Run 1).

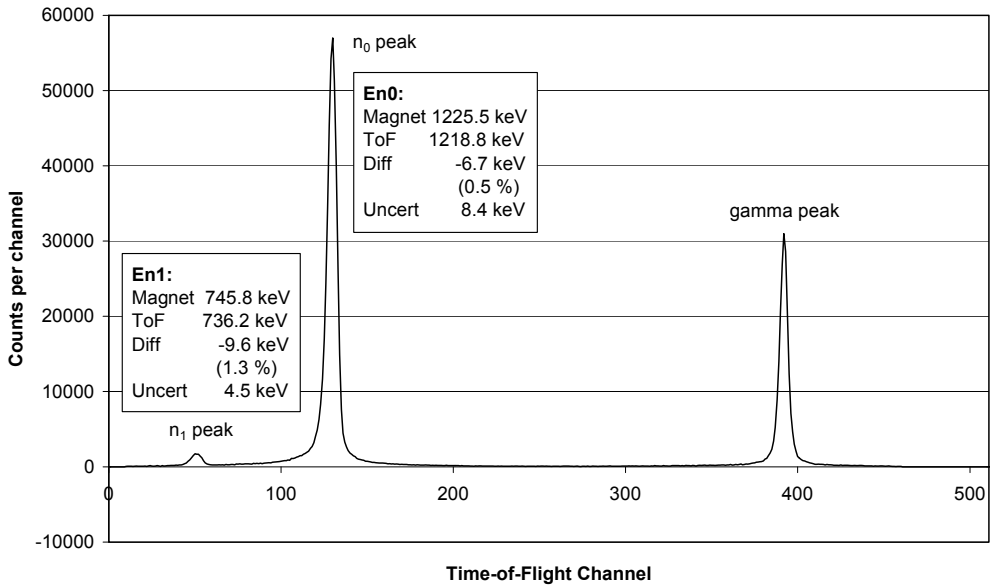

Figure 11. Corrected ToF spectrum for Run 2.

4.3 Run 3: ^{7}Li(p, n) with E_p = 2.293 MeV (E_n = 0.565 MeV)

Two days after Run 2, the accelerator was reconfigured to produce neutrons at the ISO standard energy of 565 keV from the same target.

The number of missed stop pulses was again negligible. In addition, the width of the gamma peak (Figure 12) was better than for Run 2, but no action had been specifically taken to achieve this, and the reason for the improvement remains unclear.

Figure 13 shows the neutron spectrum to be free of any gross low-energy tail. A simple analysis (subtracting in quadrature the FWHM of the gamma peak from that of the neutron peak) gives the underlying width of the neutron spectrum as $((7.31)^2 - (4.95)^2)^{1/2}$ = 5.4 channels, or 2.1 ns, which equates to 15 keV at this energy. This is considerably greater than the 5.4 keV full width usually quoted for 565 keV neutrons from this target. However, the details of the peak shapes may mean that subtraction in quadrature is not appropriate. Analysis using a program such as TARGET (see below), which calculates ToF spectra from neutron-producing targets and includes the main broadening mechanisms, should yield a more reliable figure (but see the discussion below on the problems associated with TARGET).

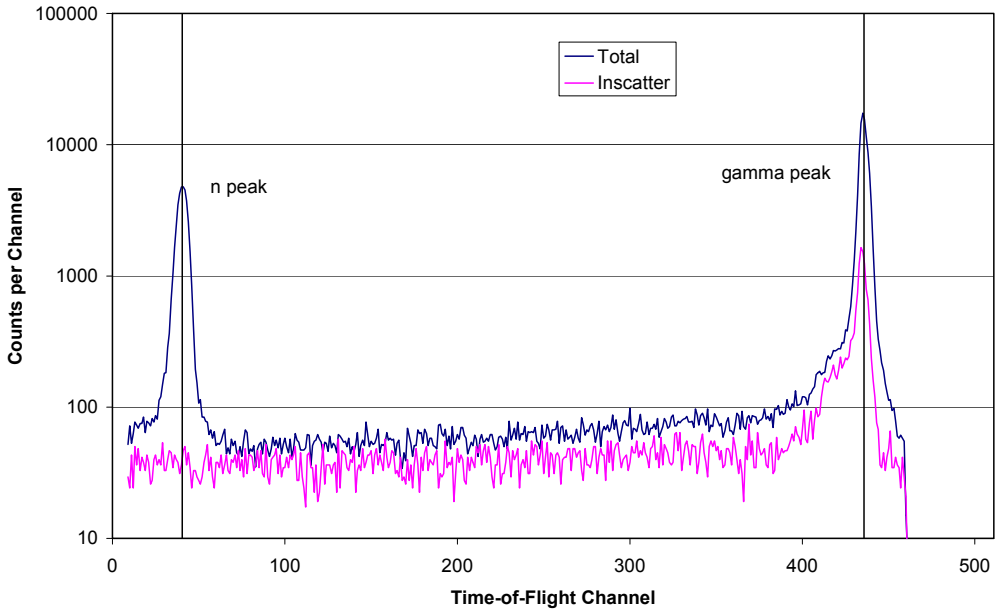

Figure 12. Total and Inscatter spectra for Run 3 (565 keV neutrons)

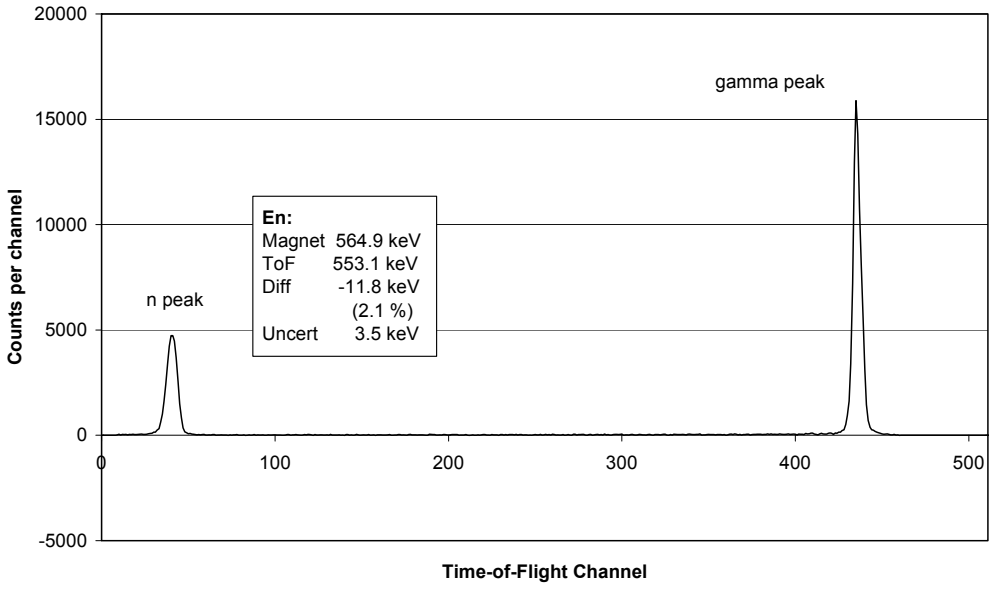

Figure 13. Corrected ToF spectrum for Run 3.

5 Analysis with the program TARGET

The Monte Carlo code TARGET[8], which originates from the Physikalisch-Technische Bundesanstalt (PTB) in Germany, is able to calculate energy and ToF spectra from several different neutron-producing targets, taking into account a number of broadening mechanisms such as the slowing down of the accelerator beam in the neutron-producing layer, the interaction of the neutrons with materials surrounding the target, and the spread of path lengths caused by the finite thickness of the detector. Run 1 was selected for detailed analysis with this program because of its good resolution and because low-energy neutrons are apparent in the corrected ToF spectrum.

A geometric model representing the structure of the NPL target assembly was drawn up using the conventions of the TARGET program. The thickness of the neutron-producing LiF layer in the target was specified as 45.1 $\mu g / cm^2$ (based on previous observations of the neutron yield curve just above the reaction threshold, which indicate an energy thickness of 5.8 keV at a beam energy of 1.881 MeV). This figure was used in preference to the nominal figure of 60 $\mu g / cm^2$ provided by the manufacturer. The energy distribution of the proton beam was specified as rectangular and extending from -2 to +2 keV relative to the nominal energy, and the energy dependence of the KL236 detector efficiency was approximated by assuming that the efficiency simply follows the $^1H(n, n)$ elastic scattering cross section. Options exist for specifying that some quantity of neutron-producing material is to be treated as having diffused into the backing, but these were not used for the present analysis.

The measured shape of the gamma peak was used as a time resolution function. This shape includes effects such as the time structure of the beam pulse and the timing resolution of the electronics. It also includes broadening due to the transit time of the gammas across the detector, which is not wanted in a resolution function for neutron peaks, but at less than 0.1 ns this broadening is negligible compared with the width of the peak (5.2 channels or 2.0 ns). The resolution function was generated from the corrected ToF data by re-binning it, using linear interpolation, to place the centre of the gamma peak at channel zero. The function was taken to 20 channels (7.9 ns) each side of the peak. In Figure 14, the derived resolution function is overlaid on the original gamma peak for comparison. A Gaussian of the same area and FWHM is also plotted, and shows that the resolution function is significantly wider than Gaussian at the base.

Because of difficulties encountered with input of a time resolution function directly into TARGET, the approach adopted was to turn off the relevant broadening mechanisms in the program and fold the resolution function into the calculated ToF spectrum afterwards.

The surprising result from initial runs was that the calculated neutron peak was about 50% wider than the measured peak. This is highly unusual; the measured width usually includes all the broadening mechanisms in the calculation plus several more. On investigating the problem by specifying very large detector thicknesses (such that this broadening mechanism dominated the others), it was found that TARGET appeared to be treating the detector as being twice as thick as the value entered. The spectrum shown below (Figure 15) was therefore calculated with the detector thickness set to half the true value (1.28 cm instead of 2.56 cm).

The vertical scale in Figure 15 is arbitrary, but the time scale is as measured and calculated, with no added time shifts. The raw TARGET spectrum, unsmeared by the resolution function, is shown in addition to the smeared spectrum.

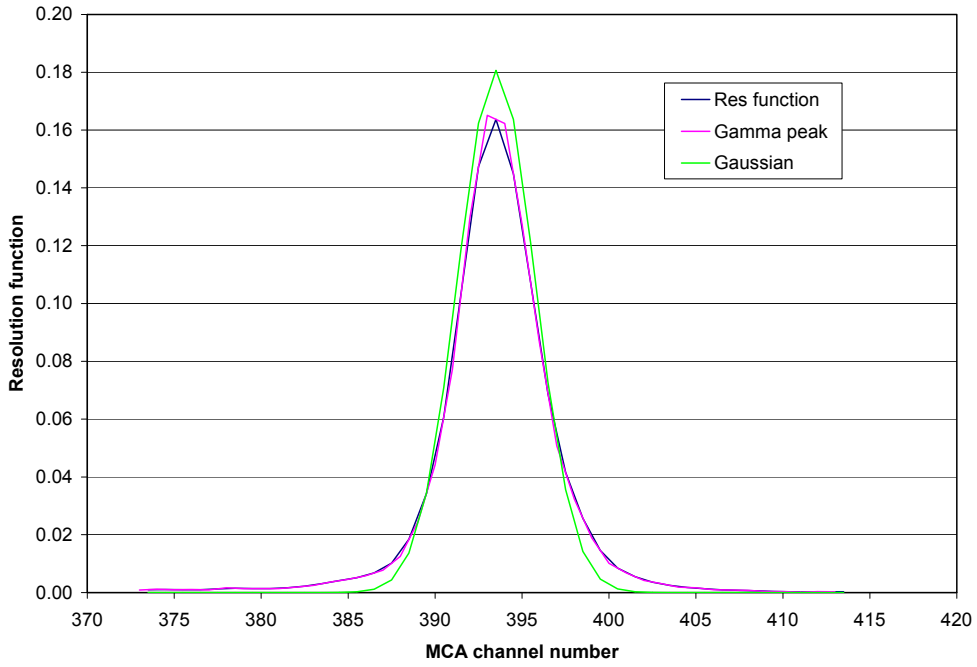

Figure 14. Resolution function for Run 1.
Also shown: the original gamma peak and a Gaussian of the same area & FWHM.

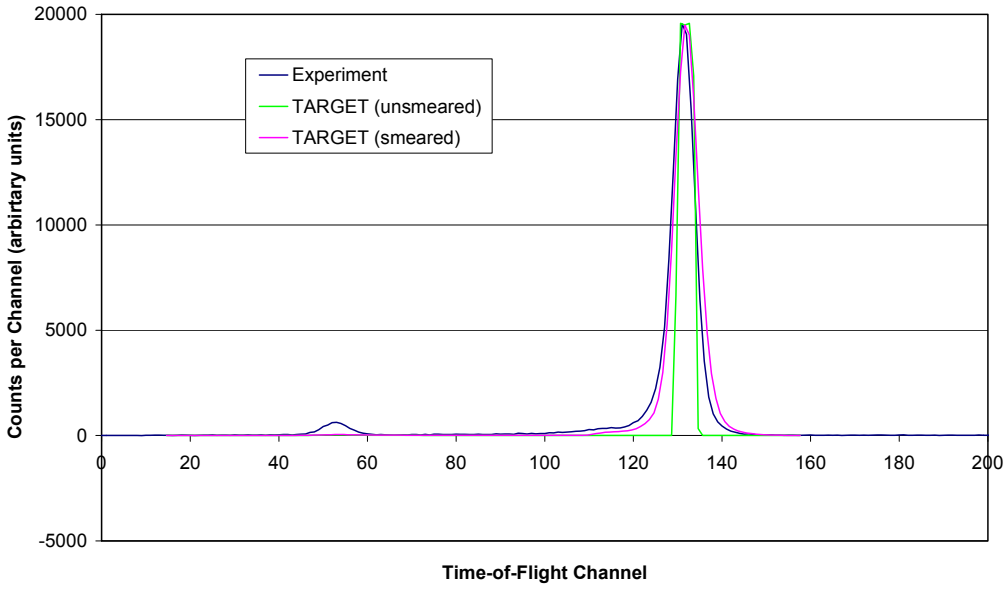

Figure 15. Measured and calculated neutron peaks for Run 1 (^{7}Li(p, n), E_p = 2.922 MeV)

The conclusions from Figure 15 are:

- Assuming the detector thickness fix adopted is correct, the 1225.5 keV neutron peak width calculated by TARGET agrees well with that measured.
- Most, but not quite all, of the low energy neutron counts seen in the measured spectrum are matched by the TARGET calculation, indicating that they come from scattering of the neutrons in the material surrounding the target.
- The remaining counts may come from lithium that has diffused into the target backing, and options exist within TARGET to explore this possibility. However, detailed studies of this kind must await resolution of the code problems described.
- TARGET does not calculate the 745.8 keV neutron peak.

6 Conclusions

The chief conclusions from this work are:

- Monoenergetic neutron spectra have been successfully measured using the NPL time-of-flight system. No gross low-energy components were observed.
- Close examination of the neutron peak shape shows a small degree of broadening due to low energy neutrons. Analysis with the TARGET program suggests that most of these are produced by scattering in the materials surrounding the target.
- Some of the low-energy neutrons may be produced by lithium that has diffused into the target backing. Detailed investigation of this must await resolution of issues with the TARGET code.
- Problems with the availability of the accelerator and the performance of the ToF system have limited its use during this programme. The performance has improved concurrently with the introduction of new beam pulser components (as described in Section 3.2) and with developments to the signal processing electronics (Sections 3.1 - 3.2).
- There remains the problem that it is difficult to set up the beam pulsing system in exactly the same way every time, and this results in a significant variation of ToF peak shapes from run to run. It is hoped that this lack of reproducibility will be overcome as greater experience is obtained with operating the system.

7 Acknowledgements

The authors are grateful to Ralf Nolte of PTB for providing the TARGET program and for sending photographs and other information on the beam pickup in use there. Thanks are also due to Dave Porter for his help in getting the best out of the Van de Graaff, and to David Thomas for reviewing the manuscript of this report. Financial support from the National Measurement System Programme Unit of the U.K. Department for Innovation, Universities and Skills is gratefully acknowledged.

8 References

1. N.P. Hawkes, A. Bennett, S.S. Cheema, N.A. Horwood, L.N. Jones, P. Kolkowski, N.J. Roberts, G.C. Taylor and D.J. Thomas, *Progress in providing neutron standards at the UK National Physical Laboratory*, Proceedings of the 10th International Symposium on Radiation Physics (ISRP 10), Nucl. Instrum. Methods in Phys. Research A **580** (2007) 183-185.
2. N. Roberts and A. Bennett, *Report on Time-of-Flight feasibility study*, September 2001, unpublished.
3. J.B. Hunt, laboratory notebook, June 1980, unpublished.
4. Andrew Corporation (3 Westbrook Corporate Center, Suite 900, Westchester, Illinois 60154, USA), HJ7-50A data sheet.
5. Huber + Suhner (UK) Ltd. (Telford Road, Bicester, Oxfordshire OX26 4LA), SX 07262 BD data sheet.
6. Wikipedia article, *RG-58* (en.wikipedia.org/wiki/RG-58).
7. M. Drosg, DROSG-2000: Neutron Source Reactions, version 2.2 (02 Jan 2003). For latest version, 2.21, see IAEA-NDS-87 Rev. 9, May 2005 (web site http://homepage.univie.ac.at/Manfred.Drosg/ drosg2000.htm).
8. D. Schlegel, *TARGET User's Manual*, Laborbericht PTB-6.42-05-2.